PROPERTIES OF THE NEUTRINO BEAMS AT A 400-GeV ACCELERATOR

Y. W. Kang

and

M. L. Stevenson
Lawrence Radiation Laboratory

February 9, 1970

I. INTRODUCTION

The present neutrino-beam design calls for a meson decay tunnel 600 meters long with a large unmoveable detector 300 meters beyond the end of it. Question: When the accelerator energy is increased to 400 GeV will there be a desire to move the target upstream in order to have a longer decay path for the more energetic mesons? How does the answer depend on neutrino energy, detector radius, the need to do high-energy $\bar{\nu}$ physics, the meson production model, the properties of the meson focusing device, and the target thickness? If the answer is likely to be yes, then there should be adequate space left between the proton beam extraction point and the 200-GeV position of the target.

II. NEUTRINO AND ANTINEUTRINO FLUX ABOVE E_ν AS A FUNCTION OF DECAY LENGTH

A. Neutrino Flux Dependence on Production Model; Detector Radius = 1.8 m

Figure 1 compares the integrated neutrino flux through a 1.8-m radius detector above E_ν = 20 GeV, 30 GeV, 40 GeV, 50 GeV, 70 GeV, and 100 GeV for the CKP[1] and HR[2] models as a function of decay length. The parameters of the CKP distribution

$$\frac{d^2 n_\pi}{dp d\Omega}_{lab} = \frac{n_\pi T}{2\pi p_0{}^2}\left(\frac{p}{T}\right)^2 e^{-p/T} e^{-p\theta/p_0}, \qquad (1)$$

where

$$n_\pi = 0.45\ E\ \ (\text{GeV})^{1/4}$$
$$T = 0.305\ E\ \ (\text{GeV})^{3/4}$$
$$p_0 = 0.22\ \text{GeV}.$$

The Hagedorn-Ranft model, modified to give agreement with the negative meson yields from Serpukhov, is described in Ref. 2. Figure 1(b) displays the respective meson momentum spectra and gives the overall K^+/π^+ ratios. One would conclude that little gain at any neutrino energy below 100 GeV is made by increasing the decay length beyond 600 meters. Only 20% gains are made at 100 GeV.

Figure 2 makes the same comparison for the flux through a 1.0-m radius detector. The conclusions are the same. Less than 10% gain is made at 100 GeV.

Figure 3 displays the differential neutrino flux averaged over detectors of 1.8 m and 1.0 meters radii. The role of the K^+ mesons in producing the most energetic neutrinos is clearly seen in this figure. Since kaons have half the proper mean-life of pions they decay in a shorter length.

B. Antineutrino Flux

In general there are fewer high-energy negative kaons than positive kaons. One might guess that the high-energy antineutrinos would come mostly from π^- decay and hence require a longer optimum decay length. Figure 4 shows this not to be the case. The shape of the $E_{\bar{\nu}} > 100$ GeV curve is very nearly the same as the corresponding one of Fig. 1. The slower moving K^-'s still contribute to the energetic antineutrinos. In Fig. 4(b) are shown the respective meson momentum spectra and the overall K^-/π^- ratios. Figure 5 is the differential antineutrino flux averaged over 1-m and 1.8-m detectors.

III. REAL FOCUSING VERSUS IDEAL FOCUSING

Intuition tells us that when the actual focusing device is used and all mesons are not moving parallel to the neutrino beam axis, the optimum decay length will be shorter than for the ideal case.

This is likely to be a small effect. For example, if the experiment is to give highest priority to say 100-GeV neutrinos, then the focusing device will be set to make those mesons that produce 100-GeV neutrinos as "perfectly" focused as possible.

To assist in the design of these focusing systems and in the design of the various experiments that will use them, we recommend that the following two dimensional histograms be output from the present "ideal focusing" neutrino flux programs. For each of the neutrino energy intervals, for which the programs now calculate a flux, output the "phase-space" histogram:

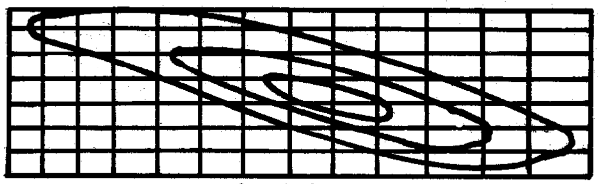

Fig. 6

These are the contour curves that will tell what shape the horn elements should take or at what currents the quadrupoles should be set.

IV. THICK-TARGET EFFECTS

Evidence from cosmic rays[3] suggests that the nucleon inelasticity is approximately 1/3, namely, that the secondary nucleon retains ≈ 2/3 the original energy of the incident nucleon. Subsequent interactions can, therefore, be an important contributor to energetic mesons. It is easy to estimate that similar meson cascades contribute only to very low energy secondary pions, i.e., the meson's inelasticity is ~4/5. Here, only the nucleon cascade is important.

Figure 7 shows how the different generations of nucleon interactions distribute themselves along the axis of the target. Details are given elsewhere.[4] Figure 8 displays the integrals of the curves of the previous figure and represent the fractions of the incident beam that ultimately interacts as an "n"th generation interaction. Previous thick-target calculations[5] were made for target thickness of 2.8 mean free paths. They did not take into account subsequent interactions.

Using the simple mnemonics described previously,[6] the neutrino spectrum is represented for each generation nucleon as a "delta function" at an energy corresponding to its canonical value

$$E_{\nu(\pi)}^{(n)} \sim \eta_{\text{proton}}^{(n)} \times (q \simeq 0.03 \text{ GeV}),$$

where
$$\eta^{(n)} = \left(\frac{2}{3}\right)^{n-1} \left[\eta^{(0)} = \frac{p_{inc}}{Mp}\right].$$

Figure 9 adds the contributions of four generations together.

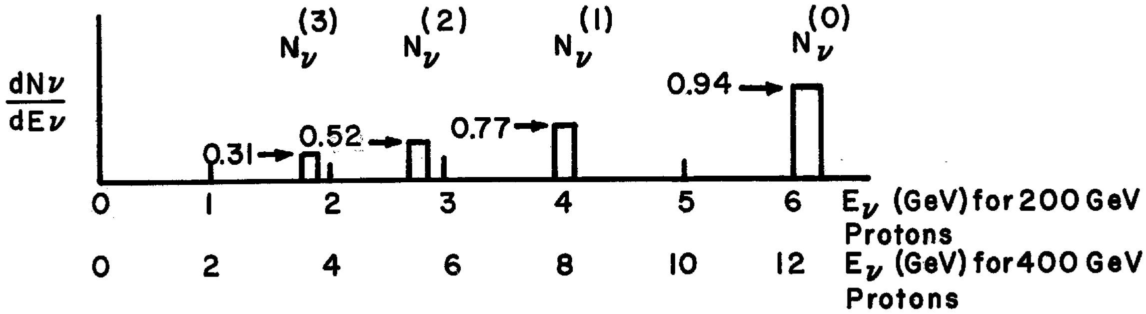

Fig. 9

Each of these delta functions has the actual shape as shown in Figs. 3 or 5. The maxima of the (1 m) curves do indeed fall at the canonical values. It is clear from the simple mnemonic that the optimum decay length optimized for $E_\nu \gtrsim 2$ GeV will be considerably shortened by inclusion of the nucleon cascades.

V. OTHER PRODUCTION MODELS

Adair[3] has described a diffraction-disassociation model for very high energy nucleon-nucleon interactions to explain certain observations in cosmic rays. It is tempting to try to extend his model down to 400 GeV and even lower. We have considered treating the fireballs of his model as distributions of bosons in thermal equilibrium with the nucleon, all contained in a volume of interaction V. If one views this volume as the volume of pionic matter at the time when the pions stop interacting with each other, i.e.,

$$V \sim \left(\frac{\hbar}{M\pi C}\right)^3 < \eta_\pi > ,$$

then one is led to a simple understanding of why the transverse momentum is observed to be nearly a constant. If the pionic energy density at that moment is taken to be

$$U(T) \approx (M\pi C^2)/(\hbar/M\pi C)^3,$$

i.e., independent of the mass of the fireball, and the temperature, a Planck-like equation, can be written

$$U(T) = \frac{M\pi C^2}{\left(\frac{\hbar}{M\pi C}\right)^3} \approx \frac{4\pi\ (kT)^4}{(2\pi\hbar)^3 C^3} \left(\int_0^\infty \frac{x^3 dx}{e^x - 1} = \frac{\pi^4}{15} \right) \qquad (1)$$

$$\left(\frac{kT}{M\pi C^2}\right)^4 = \left(\frac{30}{\pi^2}\right) \qquad (2)$$

$$kT = 0.18 \text{ GeV}. \qquad (3)$$

Inclusion of the pion rest masses in Eq. (1) makes little difference in the value for kT because of the slow variation of the fourth root of the right-hand side of Eq. (2).

One finds for a Planck-like distribution of pions of kT = 0.18 GeV and an average transverse momentum.

$$< cp_t > \approx \frac{3\pi}{4} kT = 0.42 \text{ GeV} .$$

Details of these calculations are given elsewhere.[7] Both the Adair model and our "zero-parameter" one give reasonable agreement with the charge multiplicity and the nucleon inelasticity.

We would propose that the Adair model, or a slight variation of it, be included among those already considered.[8]

The following facts should be born in mind in contemplating how the neutrino facility at 200 GeV might be modified to better use the 400-GeV protons. The pion multiplicity increases slowly with energy ($< n\pi_{ch}> = 0.45\ E_{lab}^{1/4}$) according to the CKP model while the differential spectrum is stretched by a factor of two in going from 200 GeV to 400 GeV. If all longitudinal dimensions were scaled by a factor of two, the integrated neutrino flux would be increased by only $(2)^{1/4} = 1.19$. The gain in high-energy neutrinos is obtained at the expense of the lower energy ones. The attenuation in the focusing elements will be greater at 400 GeV and will offset the gain in average multiplicity. The gains are greatest for quadrupole focusing of the highest energy neutrinos.

VI. CONCLUSIONS

The 600 meter decay length for a 300-meter shield will be adequate for the 400-GeV operation. There is little variation of the optimum decay length with detector radius, production model, or with neutrino or antineutrino requirements.

Certain thick-target effects and real focusing might lead to choosing a shorter decay length.

Another production model, that of Adair, should be considered along with those of Hagedorn-Ranft and CKP.

REFERENCES

[1]G. Cocconi, L. Koester, and D. Perkins, Lawrence Radiation Laboratory Report UCRL-10022, 1961.

[2]R. Hagedorn and J. Ranft, Nuovo Cimento 6, 169 (1968). The modified version is displayed in the paper by M. Awschalom and T. White, Secondary Particle Production at 200 GeV, National Accelerator Laboratory Report FN-191, June 9, 1969.

[3]See, for example, R. K. Adair, Phys. Rev. 172, 1370 (1968).

[4]M. L. Stevenson, Targets for the Neutrino Beam; Concepts, National Accelerator Laboratory Internal Report TM-218, February 15, 1970.

[5]Y. W. Kang and F. A. Nezrick, Neutrino Beam Design, National Accelerator Laboratory 1969 Summer Study Report SS-146, Vol. I, p. 217.

[6]M. L. Stevenson et al., The Neutrino Facility at NAL, National Accelerator Laboratory 1968 Summer Study Report B. 1-68-104, Vol. I, p. 265.

[7]M. L. Stevenson, The Role of the Planck Distribution in Understanding the Constancy of the Transverse Momentum in High Energy Nucleon-Nucleon Collisions, National Accelerator Laboratory Internal Report TM-219.

[8]See, for example, F. A. Nezrick, R. J. Stefanski, Y. W. Kang, and D. Carey, Particle Production Spectra for Neutrino Beam Design, Neutrino Task Force Report No. 1, National Accelerator Laboratory Internal Report TM-196, December 1969.

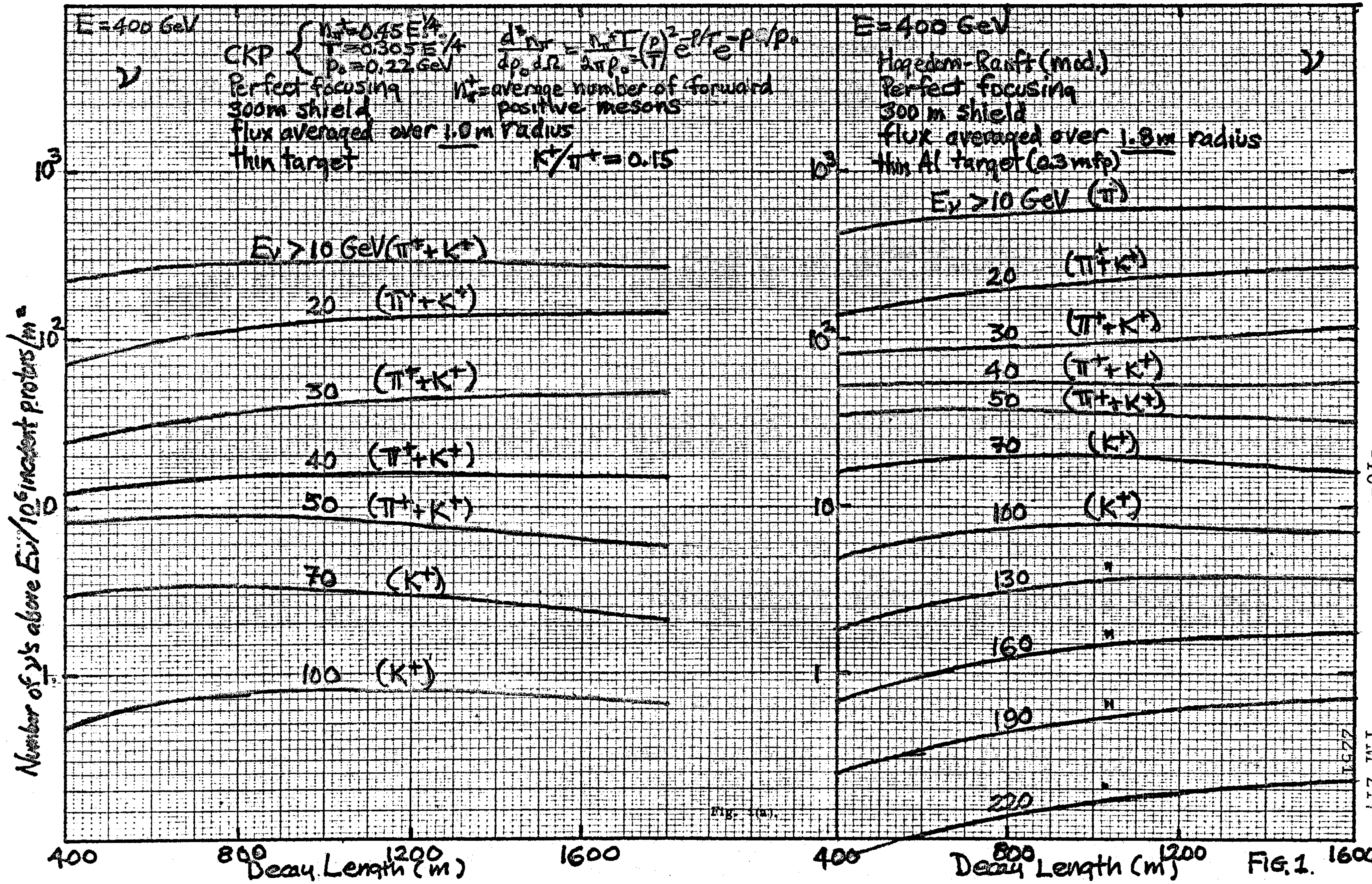
E=400 GeV
ν
CKP $\begin{cases} n_\pi^+ = 0.45\,E^{1/4} \\ T = 0.305\,E^{1/4} \\ p_0 = 0.22\text{ GeV} \end{cases}$
$\frac{d^2 n_\pi}{dp_0\, d\Omega} = \frac{n_\pi^+ T}{2\pi p_0}\left(\frac{p}{T}\right)^2 e^{-p/T} e^{-p_0/p_0}$
Perfect focusing
n_π^+ = average number of forward positive mesons
300m shield
flux averaged over 1.0 m radius
thin target
$K^+/\pi^+ = 0.15$
$E_\nu > 10$ GeV ($\pi^+ + K^+$)
20 ($\pi^+ + K^+$)
30 ($\pi^+ + K^+$)
40 ($\pi^+ + K^+$)
50 ($\pi^+ + K^+$)
70 (K^+)
100 (K^+)
Number of ν's above Eν/10⁶ incident protons/m²
10^3
10^2
10
1
400
800
1200
1600
Decay Length (m)
E=400 GeV
Hagedorn-Ranft (mod.)
ν
Perfect focusing
300 m shield
flux averaged over 1.8m radius
thin Al target (0.3 mfp)
$E_\nu > 10$ GeV (π^+)
20 ($\pi^+ + K^+$)
30 ($\pi^+ + K^+$)
40 ($\pi^+ + K^+$)
50 ($\pi^+ + K^+$)
70 (K^+)
100 (K^+)
130
160
190
220
10^3
10^2
10
1
400
800
1200
1600
Decay Length (m)

Fig. 1.

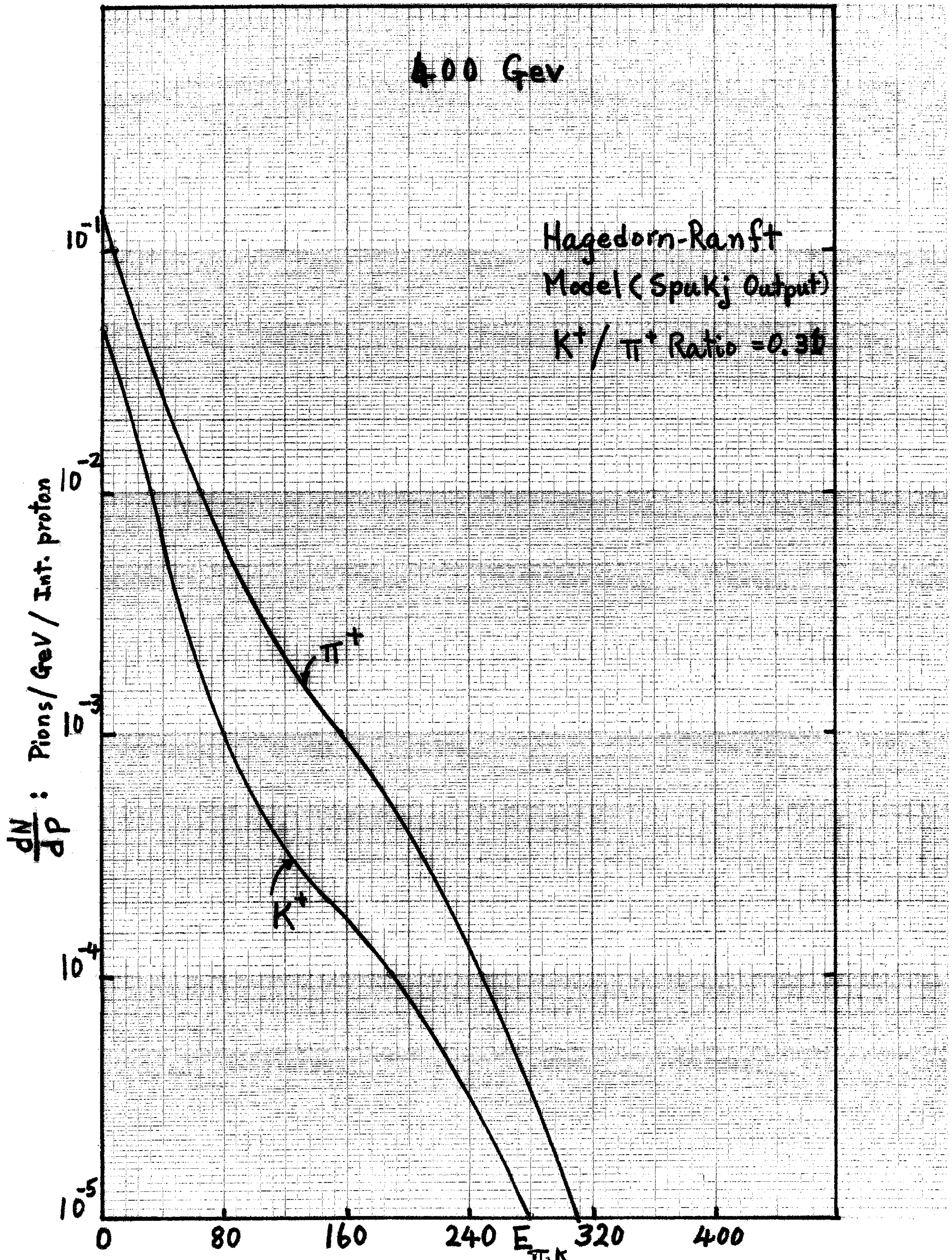
400 Gev
Hagedorn-Ranft
Model (Spukj Output)
K+/ π+ Ratio =0.31
dN/dp : Pions/GeV/Int. proton
10-1
10-2
10-3
10-4
10-5
π+
K+
0
80
160
240
320
400
E π,K

Fig 1(b)

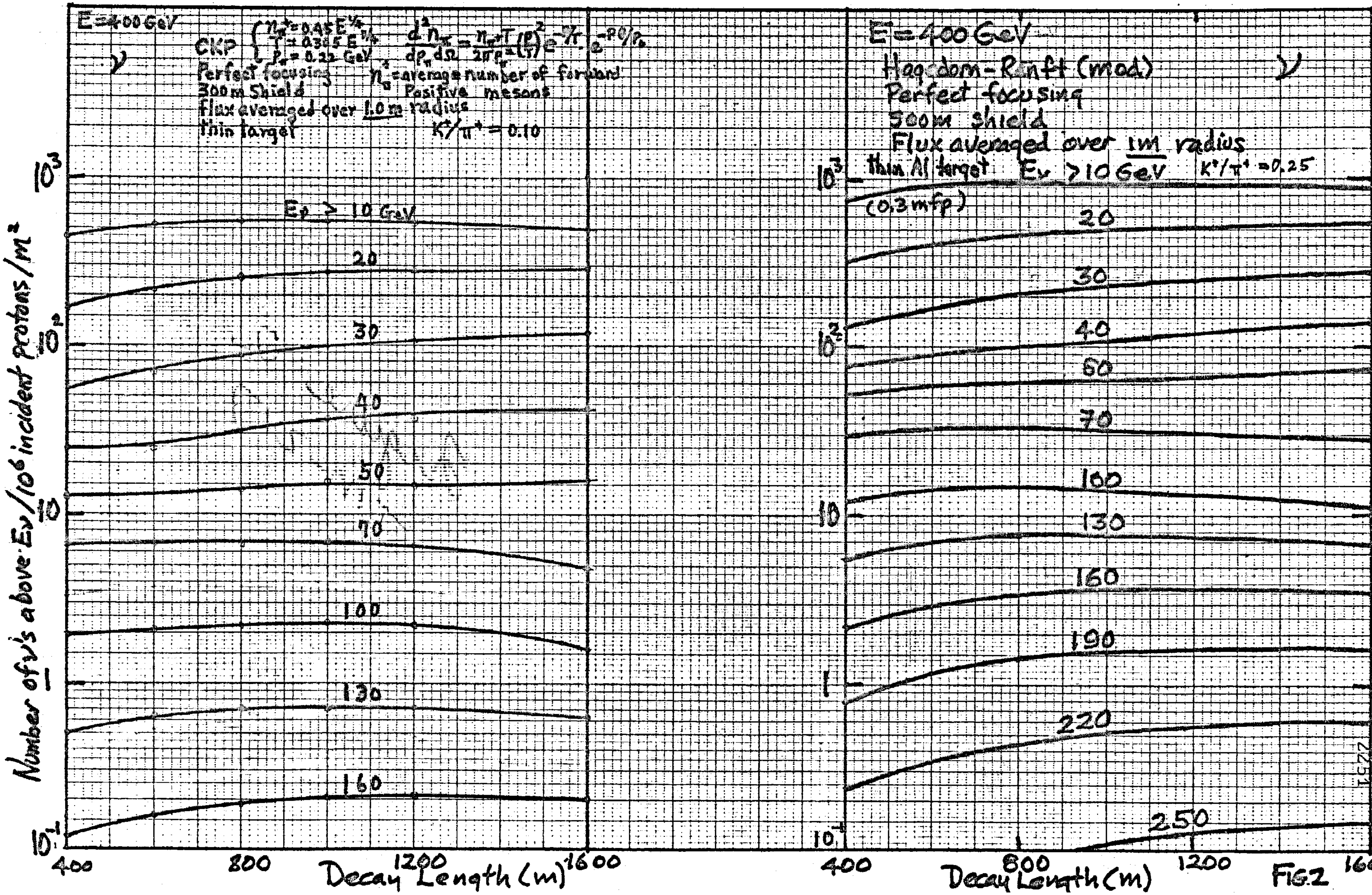
E=400 GeV
ν
CKP
Perfect focusing
300m Shield
Flux averaged over 1.0 m radius
thin target
$\bar{n}_\pi$ = average number of forward Positive mesons
K+/π+ = 0.10
Eν > 10 GeV
20
30
40
50
70
100
130
160
Number of ν's above Eν/10⁶ incident protons/m²
Decay Length (m)
E=400 GeV
Hagedorn-Ranft (mod)
Perfect focusing
500m shield
Flux averaged over 1m radius
thin Al target
(0.3 mfp)
Eν > 10 GeV
K+/π+ = 0.25
20
30
40
60
70
100
130
160
190
220
250
Decay Length (m)

FIG.2

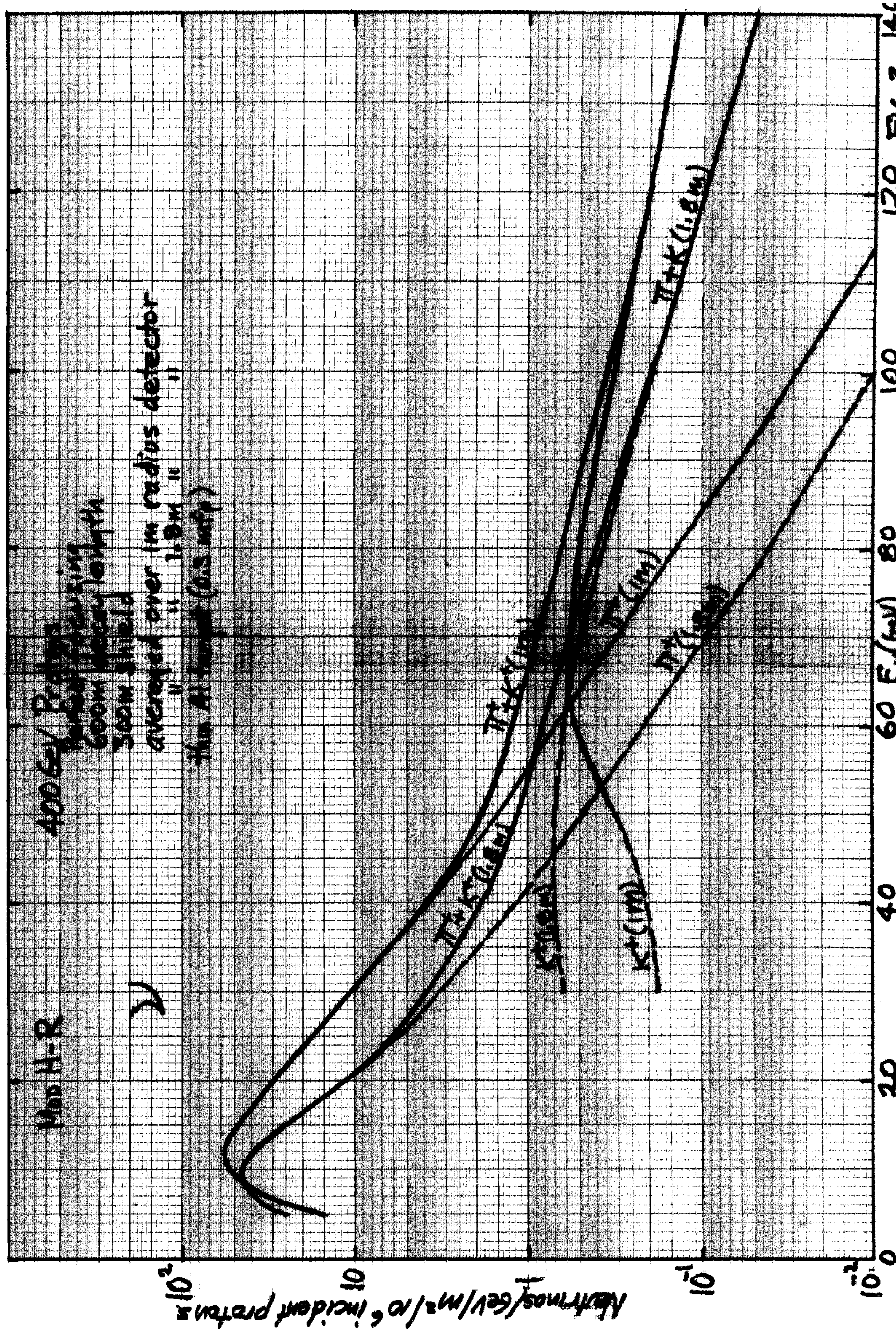
FIG. 3
400 GeV Protons
averaged over 1m radius detector
Eν(GeV)
π+K (1.8m)
π+K (1m)
K (1m)
0
20
40
60
80
100
120
140
10
1

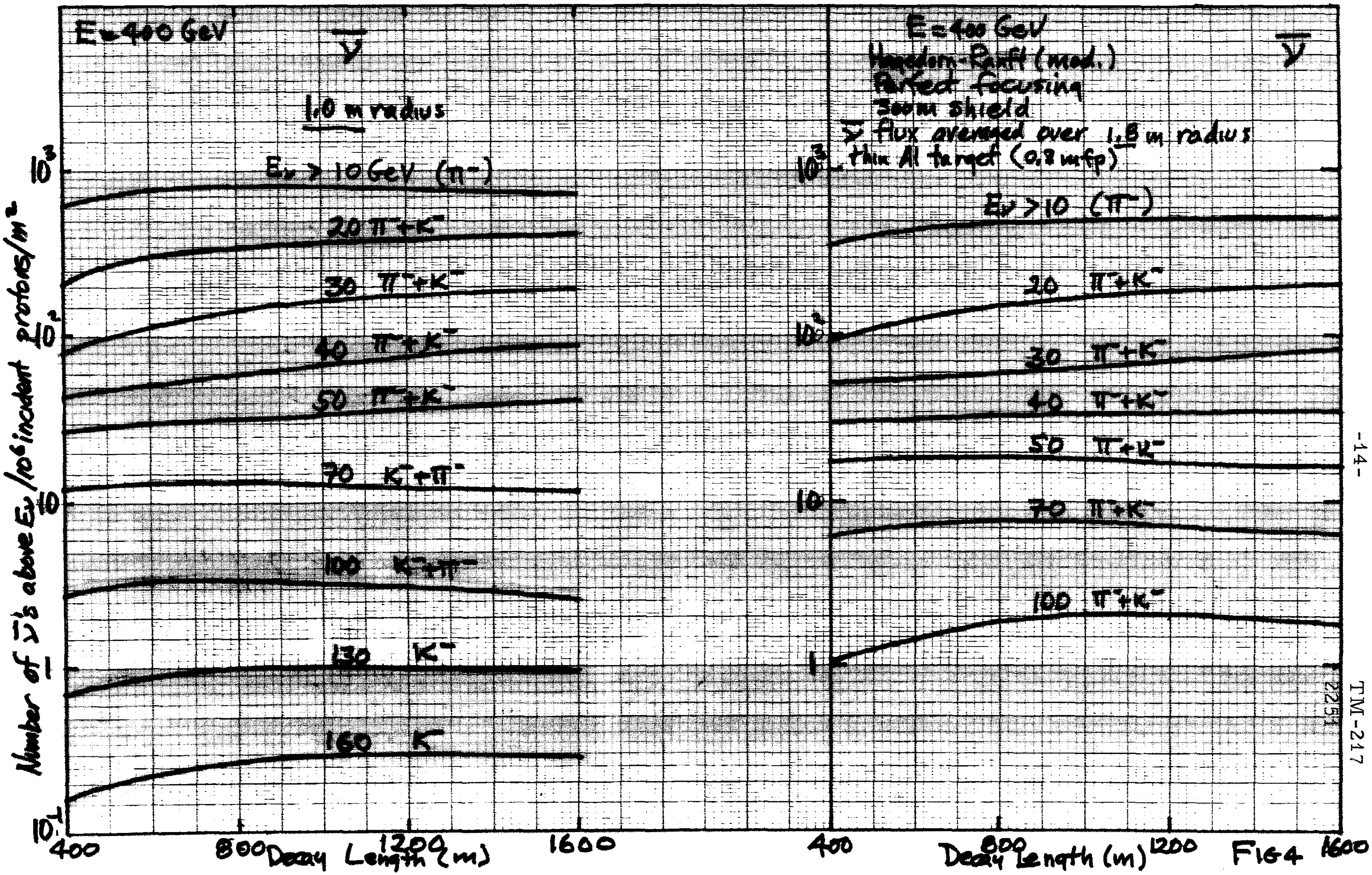

FIG 4

TM-217
2251

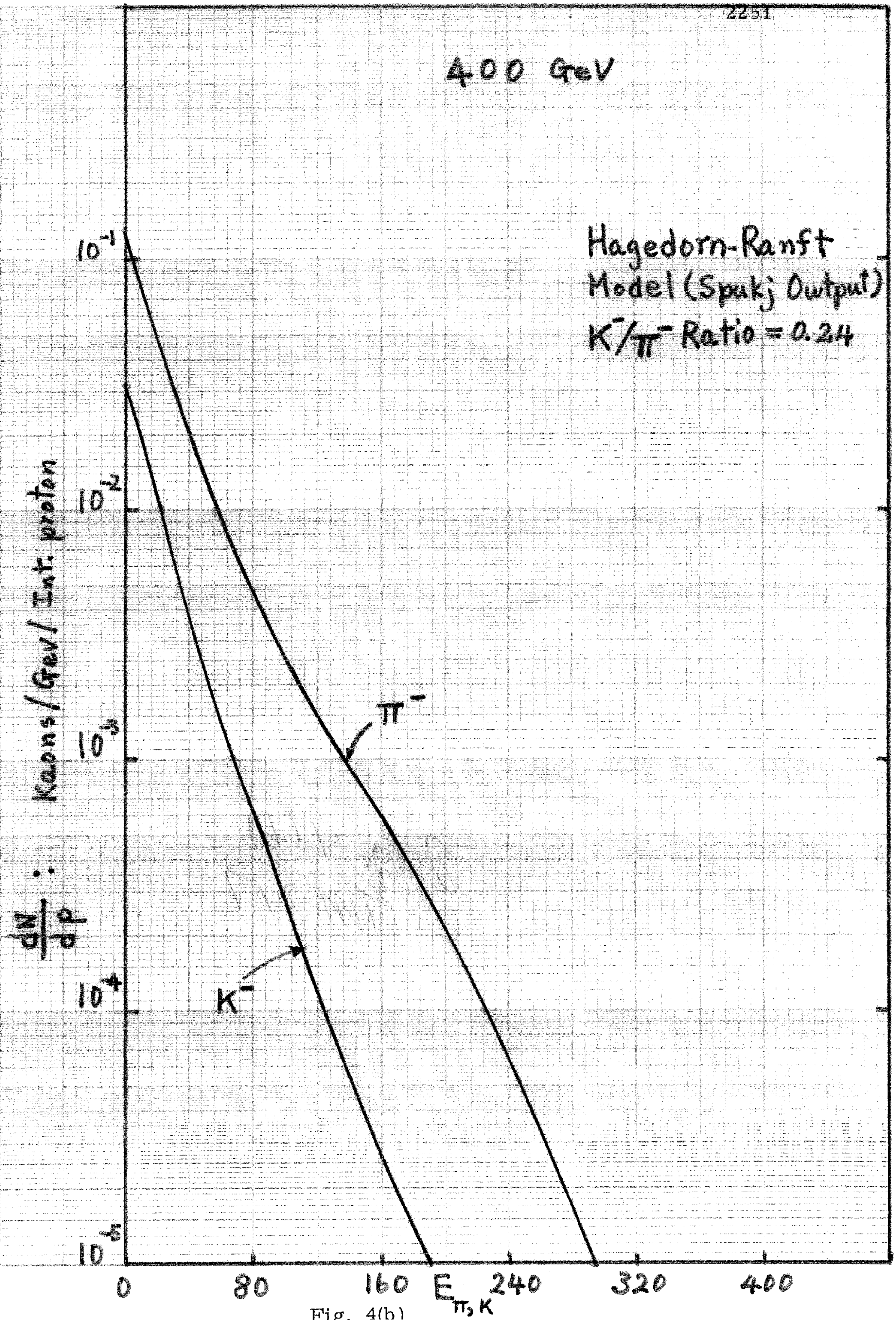
400 GeV
Hagedorn-Ranft
Model (Spukj Output)
K^-/π^- Ratio = 0.24
π^-
K^-
10^{-1}
10^{-2}
10^{-3}
10^{-4}
10^{-5}
$\frac{dN}{dp}$: Kaons/Gev/Int. proton
0
80
160
240
320
400
$E_{\pi, K}$

Fig. 4(b)

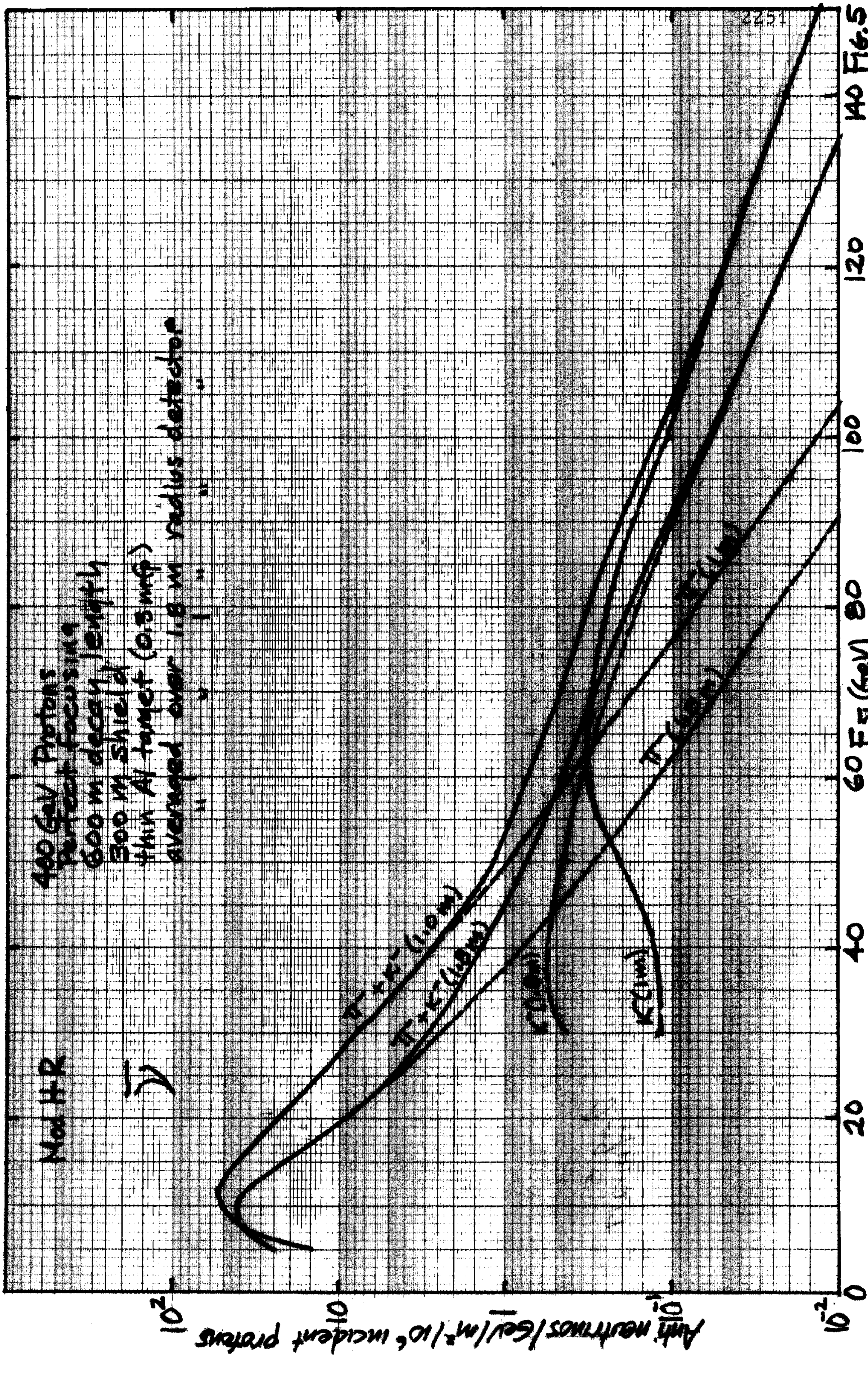
Mod H.R
400 GeV Protons
Perfect focusing
600 m decay length
300 m shield
thin Al target (0.5 mrad)
averaged over 1.8 m radius detector
π⁻+K⁻ (1.0 m)
π⁻+K⁻ (1.8 m)
K⁻(1.8 m)
K⁻(1 m)
π⁻(1 m)
π⁻(1.8 m)
Anti neutrinos/GeV/m²/10⁶ incident protons
10²
10
1
10⁻¹
10⁻²
0
20
40
60
80
100
120
140
E_ν̄ (GeV)

FIG. 5

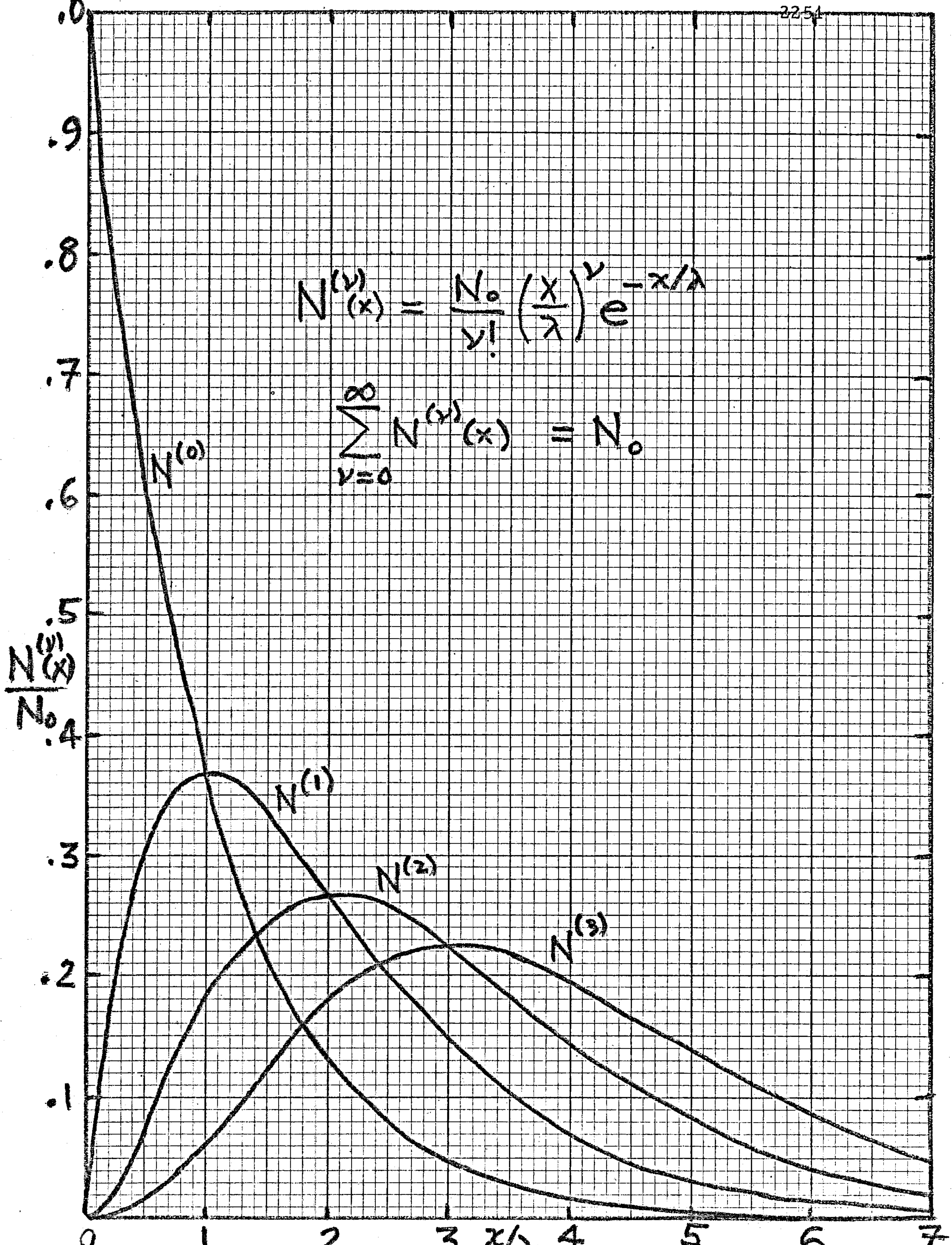
$N^{(\nu)}(x) = \frac{N_0}{\nu!}\left(\frac{x}{\lambda}\right)^{\nu} e^{-x/\lambda}$
$\sum_{\nu=0}^{\infty} N^{(\nu)}(x) = N_0$
$N^{(0)}$
$N^{(1)}$
$N^{(2)}$
$N^{(3)}$
$\frac{N^{(\nu)}(x)}{N_0}$
x/λ
.0
.9
.8
.7
.6
.5
.4
.3
.2
.1
0
1
2
3
4
5
6
7

Fig. 7

Probability of νth Generation Producing an Interaction

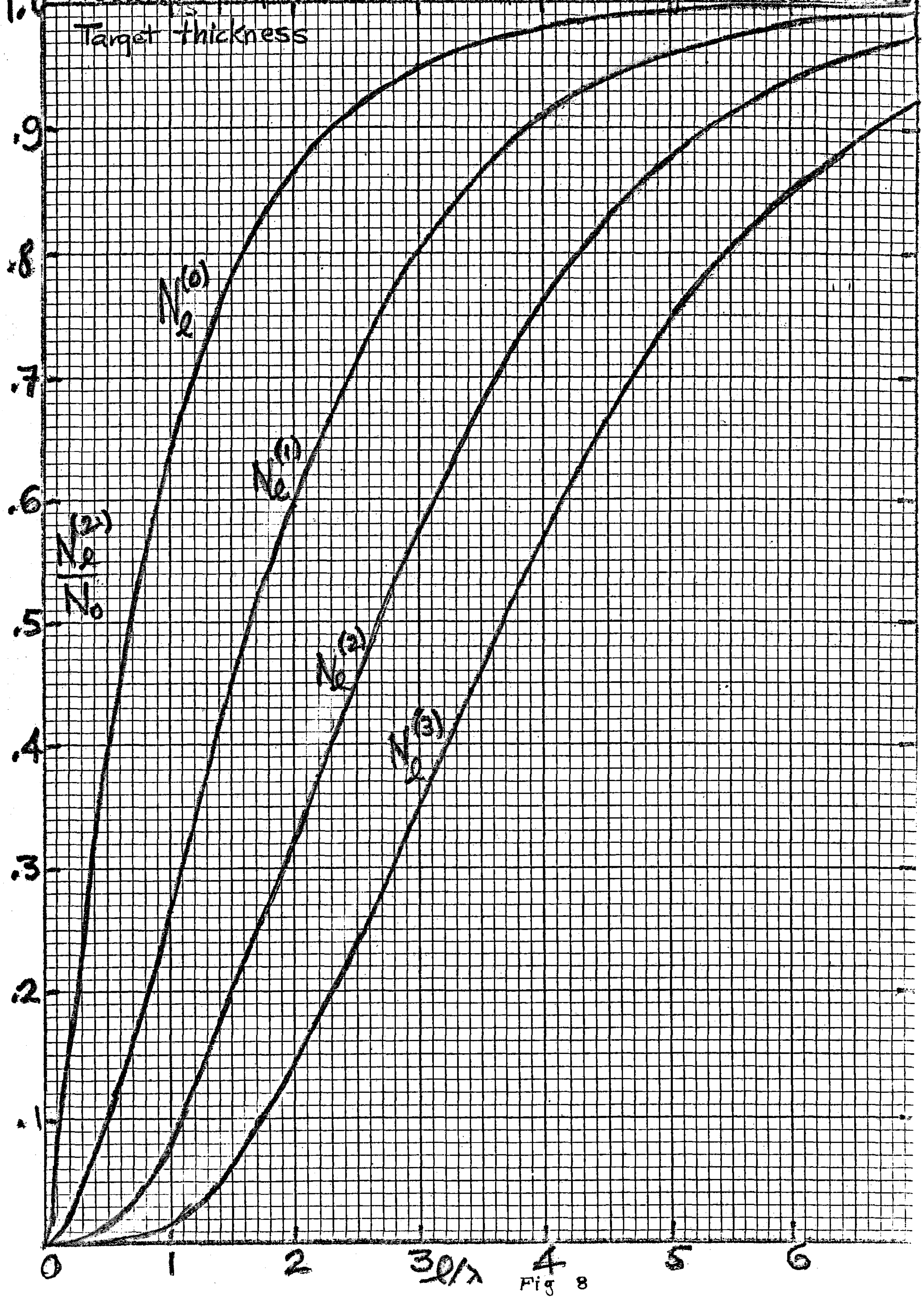

Fig 8